Sedimentary Geology 243-244 (2012) 108–116

Contents lists available at SciVerse ScienceDirect

Sedimentary Geology

journal homepage: www.elsevier.com/locate/sedgeo

Distribution of biomarkers in lacustrine sediments of the Linxia Basin, NE Tibetan Plateau, NW China: Significance for climate change ☆

Yongli Wang [a,b], Xiaomin Fang [b,c,*], Tongwei Zhang [c], Yuanmao Li [a], Yingqin Wu [a], Daxiang He [a], Yuan Gao [a], Pei Meng [a], Youxiao Wang [a]

[a] Key Laboratory of Petroleum Resources Research, Institute of Geology and Geophysics, Chinese Academy of Sciences, Lanzhou 730000, China
[b] Institute of Tibetan and Plateau Research, Chinese Academy of Sciences, Beijing 100085, China
[c] Key Laboratory of Western Resources and Environment of Education Ministry, College at Earth and Environment Sciences, University of Lanzhou, Lanzhou 730000, China

ARTICLE INFO

Article history:
Received 24 June 2010
Received in revised form 25 September 2011
Accepted 14 October 2011
Available online 21 October 2011

Editor: B. Jones

Keywords:
Biomarkers
Lacustrine sediments
Arid environmental change
Climate significance
NE Tibetan Plateau

ABSTRACT

In this study, n-alkanes, isoprenoids and n-alkyl-ketones were detected in lacustrine sediments in the Maogou section of the Linxia Basin, NE Tibetan Plateau, NW China. The distribution characteristics of these compounds correspond to arid climate change in inland Asia from the upper Oligocene to the Pliocene. The characteristic bimodal distribution of *n*-alkanes, which was observed in the investigated samples, is centered on n-C_{17}–n-C_{20} and has maximum values at n-C_{18} in all samples; n-C_{27}–n-C_{31} has maximum values at n-C_{29} in some of the samples. The front mode shows a weak even carbon number predominance of short-chain *n*-alkanes ($CPI_{17–21}$ 0.55–0.89); in contrast, the back mode has a strong odd carbon number predominance of long-chain *n*-alkanes ($CPI_{25–31}$ 1.41–2.42). Changes in the nC_{27}/nC_{31} ratio (woody plants/grassy plants) along the entire section corresponded to three climate stages: an arid to humid climate stage from ~22.5 to 18.4 Ma; 6.25 to 5.5 Ma; and two major humid stages at ~18.4 Ma and ~5.5 Ma. A warm-humid climate was identified for the ~10 Ma to ~9 Ma period, which turned to an arid-cold climate from ~8 Ma to ~7.5 Ma, by assessing changes in the $(n\text{-}C_{17}–n\text{-}C_{21})/(n\text{-}C_{27}–n\text{-}C_{31})$ ratios. Warm-humid conditions gradually increased from ~7.5 Ma to ~5.5 Ma, as has been confirmed by multiple geochemical climate indicators. A distinctive climate change toward arid-cold conditions at ~8 Ma corresponded to a striking increase in the high-carbon-numbered n-alkanes and a rapid decrease in the $(n\text{-}C_{17}–n\text{-}C_{21})/(n\text{-}C_{27}–n\text{-}C_{31})$ and $n\text{-}C_{27}/n\text{-}C_{31}$ ratios of n-alkanes, which suggests a large input of higher plants. Our observation from the biomarker analysis is in agreement with previous reports that used palynofloras to determine that climate change in the investigated region responded to the uplift of the Tibetan Plateau at ~8 Ma.

1. Introduction

The use of molecular fossils to reconstruct paleoclimate and paleoenvironment has attracted increasing attention and has become an important part of molecular stratigraphy (Fu and Sheng, 1992, 1996; Street Perrott et al., 1997; Evershed et al., 1999; Sheng et al., 1999; Zhang et al., 1999). Molecular fossils are stable compounds, are preserved for long time-periods and are distributed widely, characteristics that qualify them as good indicators of climatic and environmental changes. In addition, molecular fossils provide excellent information on the origin of parent materials, the redox degree of organic matter, the growth status of microorganisms in ancient environments, the different ecological and vegetation systems, certain climate conditions and the thermal evolution of organic matter. Many types of biomarkers have been reported, such as alkanes, aromatics, alkanoic acids, alkanols, alkenones, esters and other rare and special compounds, which can be used to record climate change (Gonzalez-Vilia et al., 2003; Xie et al., 2003a, 2003b, 2003c; Wang et al., 2005, 2006, 2007; Bai et al., 2006a, 2006b). The research targets have included aerosols (Simoneit et al., 1991), marine sediments (Volkman et al., 1995; Pearson and Mcnichol, 2001; Lu et al., 2005), lacustrine and peat deposits (Thiel et al., 1997; Zhang et al., 1999; Xie and Evershed, 2001), glaciers (Xie et al., 1999), ancient vegetation (Mitra et al., 2000), loess (Yan et al., 1998; Xie et al., 2002, 2003a; Wang et al., 2004), a cave stalagmite (Xie et al., 2003b), estuarine sediments (rocks) (Gonzalez-Vilia et al., 2003; Greenwood and Arouri, 2003) and the shell bar of a salt lake (Zhang et al., 2007).

Northwestern China is mainly made up of large inland basins that accumulated within extra-thick Cenozoic sediments. Many researchers have understood the value of these sediments and have conducted

☆ Supported by the CAS Strategic Priority Research Program Grant Nos. XDA05120204, 2012CB214701, the Knowledge Innovation Program of the Chinese Academy of Sciences (Grant Nos. KZCX2-EW-104, KZCX2-YW-Q05-05, KZCX2-YW-104) and the NSFC (Grant Nos. 41172169, 40672123).

* Corresponding author at: Postal address: No.18 Shuangqin Road, Haidian District, Beijing, 10085, PR China. Tel.:+86 13501137997; fax: +86 931 4960828.
E-mail address: fangxm@itpcas.ac.cn (X. Fang).

0037-0738/$ – see front matter © 2011 Elsevier B.V. All rights reserved.
doi:10.1016/j.sedgeo.2011.10.006

chronostratigraphic work to obtain a record of arid environmental changes in inland Asia. Li (1995) and Fang et al. (1999, 2003) established a chronological sequence for the Linxia Basin. Their studies provide a detailed magnetostratigraphic record of subsidence in the Linxia Basin. Based on their research, we know that deposition in the Linxia Basin began at 29 Ma and continued nearly without interruption until 1.7 Ma. Studies of palynofloras and sedimentary chemistry have shown that the climate was characterized by dry conditions during the late Oligocene and warm-humid conditions during the early and middle Miocene; these studies concluded that the climate has been under drier conditions since 8 Ma (Li and Fang, 1998; Ma et al., 1998). However, studies of carbon and oxygen isotopes of carbonate indicate that the most important climatic changes happened at ~12 Ma and that the arid climatic conditions became obvious from ~9.6 to 8.2 Ma (Dettman et al., 2003). A carbon isotopic study of mammalian tooth fossils revealed that C4 grassy plants were not a significant part of the ecosystem in the Linxia Basin until 2–3 Ma. In addition, sudden increases in oxygen isotope ratios have been related to arid climatic conditions at 7 Ma (Wang and Deng, 2005). Aeolian dust accumulation reflects the history of aridification in Northwest China; however, the accepted record of aeolian red clay begins at only approximately 7–8 Ma ago (Sun et al., 1998; Ding et al., 1999; Song et al., 2001; An et al., 2002). Although the red clay in Qin'an has been dated back to 22 Ma (Guo et al., 2002), its dating requires further study. These studies show that the records of different environmental proxies for arid climatic changes in inland Asia have given different results.

Sediments in the Linxia Basin are rich in lipids and have weak diagenesis; therefore, they are an ideal recorder of arid climatic changes. These sediments' biomarkers should record the evolution of arid climate in Northwest China. In this study, we make an exploratory attempt to determine the distribution characteristics of biomarkers in the sediments of the Linxia Basin in hopes of revealing the process that governs arid environmental changes and understanding whether that process responded to the uplift of the Qinghai–Tibetan Plateau.

2. Geologic background and the division of palynofloras

The Linxia Basin is located at the northeastern edge of the Tibetan Plateau (102°30′~104°E, 35°10′~35°51′N, Fig. 1). The sedimentary rocks of the Linxia Basin are dominated by mudstone and sandstone of fluvial and lacustrine origin (Table 1). The Maogou section, in the central part of the Linxia Basin, is representative of the Tertiary red bed. Li Jijun and Fang Xiaomin et al. have established a chronological sequence of the Linxia Basin (Li, 1995; Fang et al., 2003). Their study provides a detailed magnetostratigraphic record of subsidence in the basin. The red bed in this area is from 30.6 to 4.0 Ma, that is, from the upper Oligocene to the Pliocene, and it is a continuous sedimentary section whose total thickness is 443 m. Ma and colleagues (Li and Fang, 1998; Ma et al., 1998) obtained statistics based on vegetation studies showing that the Maogou section in the east of the Linxia Basin can be divided into six important climatic events (Fig. 2) and four major stages (A–D, Fig. 2), including seven palynological assemblage zones (I–VII, Fig. 2).

3. Sampling and experiments

3.1. Sampling

Twelve representative lacustrine sediment samples were collected from bottom to top from 30.6 Ma to 4.50 Ma, respectively, in the 443-m-thick section. Table 1 shows the thickness, lithology of each sample and Fig. 2 shows the location of each sample in the studied section.

3.2. Sample pretreatment and GC-MS analysis

Two hundred and fifty grams of the soil sample were air-dried and ground to particles larger than 100 mesh that were extracted continuously for 70 h with chloroform in a Soxhlet extractor. The concentrated extracts weighed 5–10 mg. To prevent the loss of components, such as saturated hydrocarbon and oxygenated compounds, a silica gel-

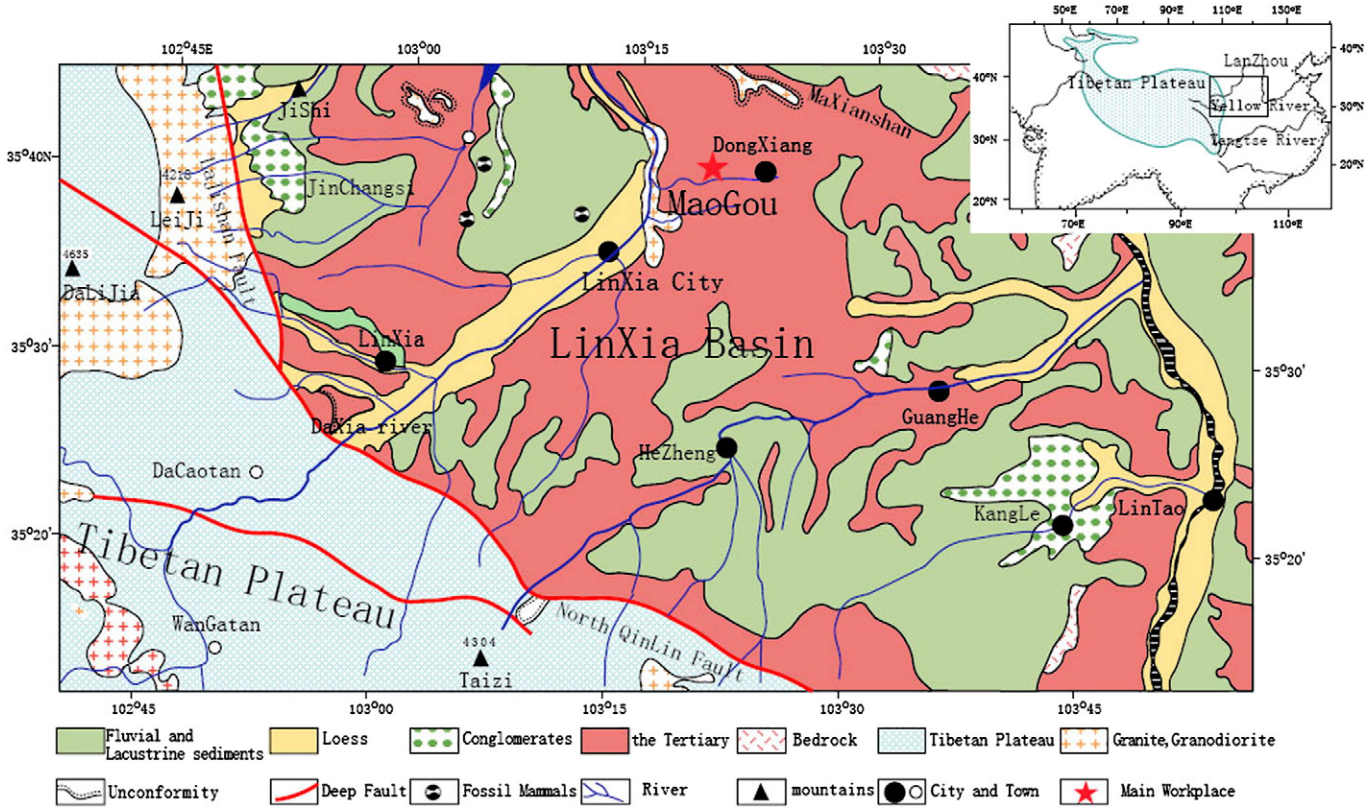

Fig. 1. Location of the study area. The map shows the Tibetan Plateau and Maogou section.

Table 1
Classification of Lithofacies and geochemical parameters of the Maogou section (30.6–4.4 Ma) in the Linxia Basin.

N-alkanes									Isoprenoids			
Sample #	Thickness/m	Lithology	The distribution range of alkanes	The main Peak of alkanes	CPI_{17-21}[a]	CPI_{23-31}[b]	CPI_{25-31}[c]	nC_{27}/nC_{31}	nC_{17-21}/nC_{27-31}	Pr/Ph	Pr/nC_{17}	Ph/nC_{18}
MG-12	431	Brown-lacustrine mudstone	nC_{16}–nC_{32}	nC_{18}	0.62	1.31	1.61	1.00	4.11	0.53	0.42	0.37
MG-11	397	Brown-lacustrine mudstone	nC_{16}–nC_{32}	nC_{18}	0.64	1.86	2.33	1.80	4.46	0.52	0.47	0.43
MG-10	368	Brown-lacustrine sandstone	nC_{16}–nC_{32}	nC_{18}	0.55	1.30	1.59	0.95	3.47	0.33	0.50	0.37
MG-9	320	Brown-block mudstone	nC_{16}–nC_{32}	nC_{18}, nC_{29}	0.57	1.48	1.70	0.97	1.51	0.37	0.58	0.47
MG-8	318	Brown-block mudstone	nC_{16}–nC_{32}	nC_{18}	0.60	1.33	1.64	0.88	5.34	0.36	0.37	0.37
MG-7	289.8	Amaranth mudstone	nC_{16}–nC_{32}	nC_{18}, nC_{29}	0.74	1.77	2.04	0.84	1.80	0.36	0.36	0.36
MG-6	273	Amaranth mudstone	nC_{16}–nC_{32}	nC_{18}, nC_{29}	0.67	1.37	1.57	0.94	1.83	0.40	0.39	0.41
MG-5	233.8	Maroon-lacustrine mudstone	nC_{16}–nC_{32}	nC_{18}	0.71	1.83	2.17	0.78	4.03	0.50	0.53	0.43
MG-4	180.6	Maroon mudstone	nC_{16}–nC_{32}	nC_{18}, nC_{29}	0.82	1.41	1.65	0.92	1.94	0.46	0.57	0.64
MG-3	136.2	Maroon mudstone	nC_{16}–nC_{32}	nC_{18}, nC_{29}	0.89	1.26	1.41	1.40	1.07	0.33	0.91	1.13
MG-2	74.9	Lacustrine mudstone	nC_{16}–nC_{32}	nC_{18}, nC_{29}	0.62	2.01	2.42	0.51	1.31	0.39	0.71	0.61
MG-1	29.55	Fluvio-lacustrine sandstone	nC_{16}–nC_{32}	nC_{18}	0.75	1.43	1.69	0.88	2.14	0.53	0.51	0.59

[a] $CPI_{17-21} = 0.5 \times [((n\text{-}C_{17} + n\text{-}C_{19} + n\text{-}C_{21})/(n\text{-}C_{16} + n\text{-}C_{18} + n\text{-}C_{20})) + ((n\text{-}C_{17} + n\text{-}C_{19} + n\text{-}C_{21})/(n\text{-}C_{18} + n\text{-}C_{20} + n\text{-}C_{22}))]$.
[b] $CPI_{23-31} = 0.5 \times [((n\text{-}C_{23} + n\text{-}C_{25} + n\text{-}C_{27} + n\text{-}C_{29} + n\text{-}C_{31})/(n\text{-}C_{22} + n\text{-}C_{24} + n\text{-}C_{26} + n\text{-}C_{28} + n\text{-}C_{30})) + ((n\text{-}C_{23} + n\text{-}C_{25} + n\text{-}C_{27} + n\text{-}C_{29} + n\text{-}C_{31})/(n\text{-}C_{22} + n\text{-}C_{24} + n\text{-}C_{26} + n\text{-}C_{28} + n\text{-}C_{30} + n\text{-}C_{32}))]$.
[c] $CPI_{25-31} = 0.5 \times [((n\text{-}C_{25} + n\text{-}C_{27} + n\text{-}C_{29} + n\text{-}C_{31})/(n\text{-}C_{24} + n\text{-}C_{26} + n\text{-}C_{28} + n\text{-}C_{30})) + ((n\text{-}C_{25} + n\text{-}C_{27} + n\text{-}C_{29} + n\text{-}C_{31})/(n\text{-}C_{26} + n\text{-}C_{28} + n\text{-}C_{30} + n\text{-}C_{32}))]$.

alumina chromatographic column was not used for the separation of group components. After drying at 20 to 25 °C, the sample was diluted with chloroform, then all of its components underwent GC-MS analysis.

The analysis of biomarkers was carried out at the Key Laboratory of Gas Geochemistry, Institute of Geology and Geophysics, Chinese Academy of Science. The GC-MS analysis was performed using an

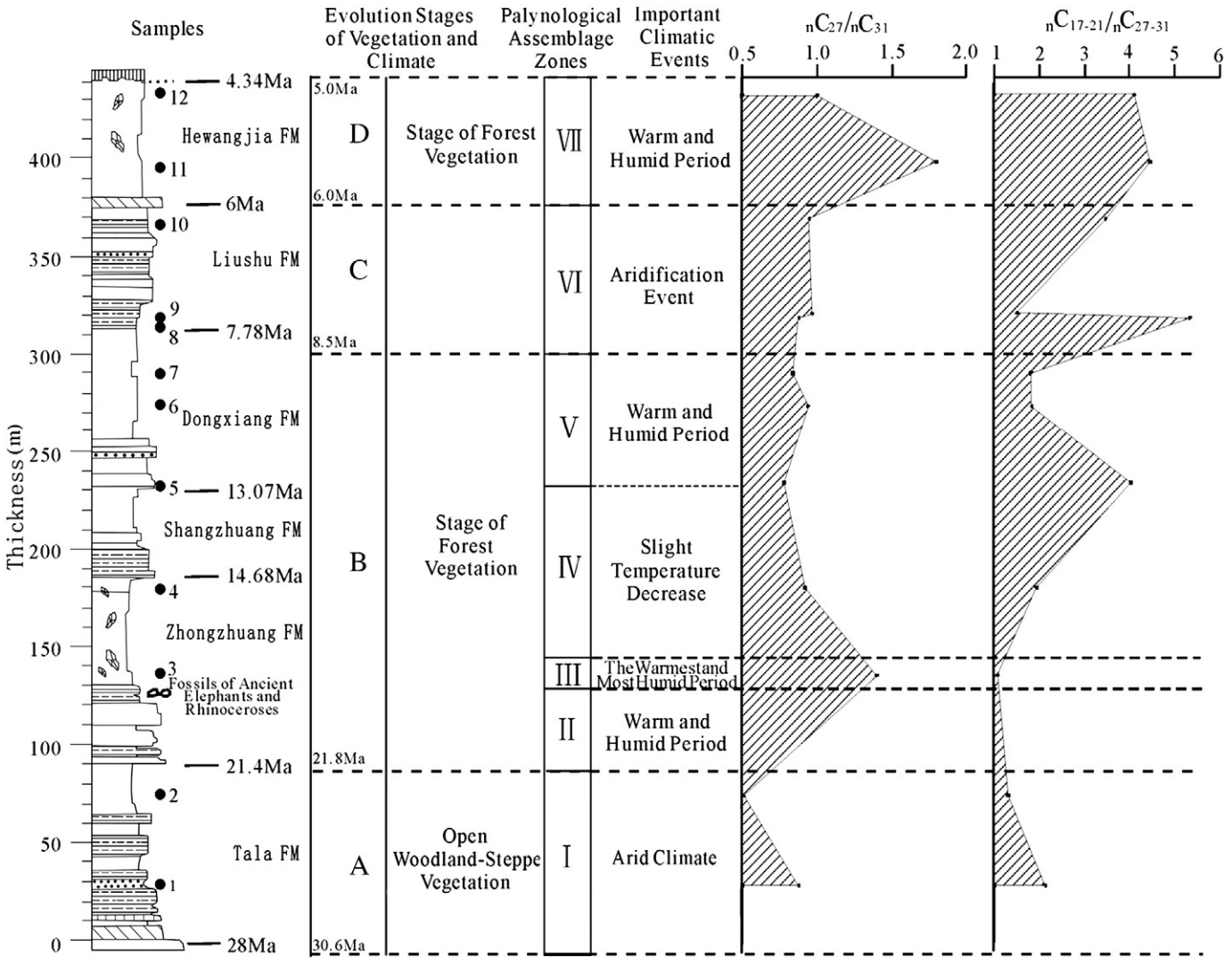

Fig. 2. The comparison between biomarkers and palynological analyses.

HP 5973 MSD (Aglient Technologies, Wilmington, DE, USA) interfaced to an HP 6890 gas chromatograph that was fitted with a 30 m × 0.25 mm i.d. fused silica capillary column coated with a film (0.25 μm) of 5% phenyl-methyl-DB-5. For routine GC analysis, the oven was programmed from 80 to 300 °C at 3 °C/min with an initial and source temperature of 230 °C and an electron multiplier voltage of 1900 V over the range of 35–550 Da.

4. Results and discussion

4.1. Distribution characteristics of n-alkanes and isoprenoids as well as climate implications

Abundant n-alkanes and isoprenoids were detected in all 12 samples. The mass chromatograms of the n-alkanes of the samples are shown in Fig. 3. The n-alkanes showed a bimodal distribution throughout the depositional section. The characteristic bimodal distribution of *n*-alkanes, which was observed in the investigated samples, is centered on *n*-C_{17}–*n*-C_{20} and has maximum values at *n*-C_{18} in all samples; and *n*-C_{27}–*n*-C_{31} has maximum values at *n*-C_{29} in some of the samples (MG1, MG2, MG3, MG4, MG6, MG7). The front mode shows a weak even-carbon-number predominance of short-chain *n*-alkanes (CPI_{17-21} 0.55–0.89); in contrast, the back mode has a strong odd-carbon-number predominance of long-chain *n*-alkanes (CPI_{25-31} 1.41–2.42). The distribution of n-alkanes in the samples ranged from n-C_{17} to n-C_{32}, with an obvious maximum peak at n-C_{18} throughout the entire section. This result suggests that the organic matter in the sedimentary section shared the same major source.

In general, the increase in the relative abundance from n-C_{27} to n-C_{31} of the high-carbon-numbered n-alkanes suggests that higher

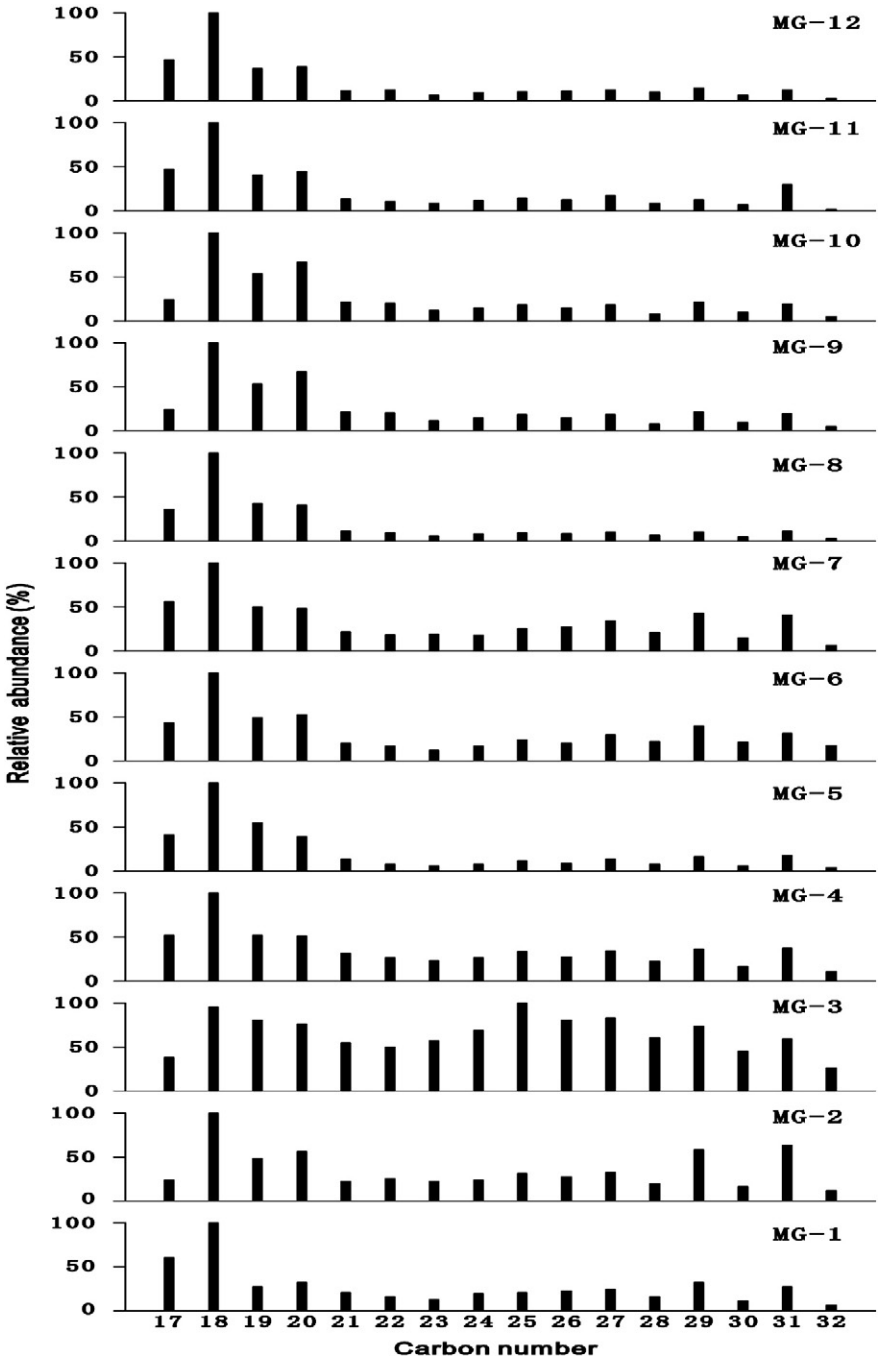

Fig. 3. The distribution of n-alkanes in all 12 samples.

plants were the dominant contributor to the organic matter in the Linxia Basin. A relatively large input of higher plants may have corresponded to a cold or dry climate change, which could have been recorded in the sedimentary section. The distribution of n-alkanes, therefore, is characterized by a striking increase in the relative abundance from n-C_{27} to n-C_{31} of high-carbon-numbered n-alkanes from MG5 to MG6 and MG8 to MG9 at ~13 Ma and ~8 Ma, respectively. This increase may be related to large inputs of higher plants when the distinct change to cold and arid conditions occurred. Our observation from the biomarker analysis is in agreement with previous reports that used palynofloras to determine an aridification event at ~8 Ma (palynological assemblage zone VI, Fig. 2).

The ratios of $(nC_{17}–nC_{21})/(nC_{27}–nC_{31})$ (bacteria and algae/higher plants) is an indication of relative climate change from warm-humid to arid-cold (Xie et al., 1999, 2003a, 2003b, 2003c; Xie and Evershed, 2001; Wang et al., 2002). As shown in Fig. 2 and Table 1, six stages of climate change were revealed in the entire section, which was based on organic geochemical parameters. Three of these stages, including ~18.4 to 13 Ma, ~9 to 8 Ma and ~7.5 to 5.5 Ma, showed a gradual increase in the ratio of $(nC_{17}–nC_{21})/(nC_{27}–nC_{31})$ within the continuous sediments, which suggests relatively constant warm-humid climate conditions in the deposition of MG3 to MG5, MG7 to MG8 and MG9 to MG11, respectively. The dominant contribution to the organic matter was from bacteria and algal organisms. From ~25.8 to 18.4 Ma, ~13 to 10 Ma and ~8 to 7.5 Ma, the ratio of $(nC_{17}–nC_{21})/(nC_{27}–nC_{31})$ decreased gradually within the continuous sediments, which suggests relatively arid-cold climate conditions in the deposition of MG1 to MG3, MG5 to MG6 and MG8 to MG9, respectively. Higher plants were likely the main source of organic matter input during those three stages. A rapid change (5.34 to 1.51, Table 1) in $(nC_{17}–nC_{21})/(nC_{27}–nC_{31})$ ratios occurred for MG8 to MG9 at ~8 Ma, which indicates an abundant higher plant input when the distinct change to a dry climate at ~8 Ma occurred. Our results agree with previous observations about the desertification of central Asia, which was dated to approximately 8 Ma at the eastern Loess Plateau (Ding et al., 1999). A similar observation of the aridification event at ~8 Ma (palynological assemblage zones VI, Fig. 2) was made by Ma et al. (1998) using palynofloras.

Evidence of modern molecular organic geochemistry shows that the ratio of nC_{27}/nC_{31} n-alkanes is indicative of woody plants and grassy vegetation (Cranwell et al., 1987; Meyer and Ishiwatari, 1993; Xie and Evershed, 2001; Xie et al., 2003c). A high ratio of $nC_{27}–nC_{31}$ indicates a greater input of woody plants and more humid conditions. As shown in Fig. 2, the ratio of nC_{27}/nC_{31} increased for MG2 to MG3 and MG10 to MG11 from ~22.5 to 18.4 Ma and ~6.25 to 5.5 Ma, respectively. This increase suggests that the woody plant input was dominant in the above sediments under relatively continuous humid climate conditions. The maximum ratios of n-C_{27}/n-C_{31} for MG3 and MG11 (at ~18.4 Ma and ~5.5 Ma, respectively), suggest two major humid stages of climatic change in the whole section. These observations are similar to the warmest and most humid (palynological assemblage zones III, Fig. 2) and the warm and humid (palynological assemblage zones III, Fig. 2) stages determined by analyzing the palynofloras. Note that in Fig. 3, there is an important feature of the n-alkane distributions: the singular dominance from nC_{23} to nC_{27} of mid-chain components in MG3. This distribution is representative of

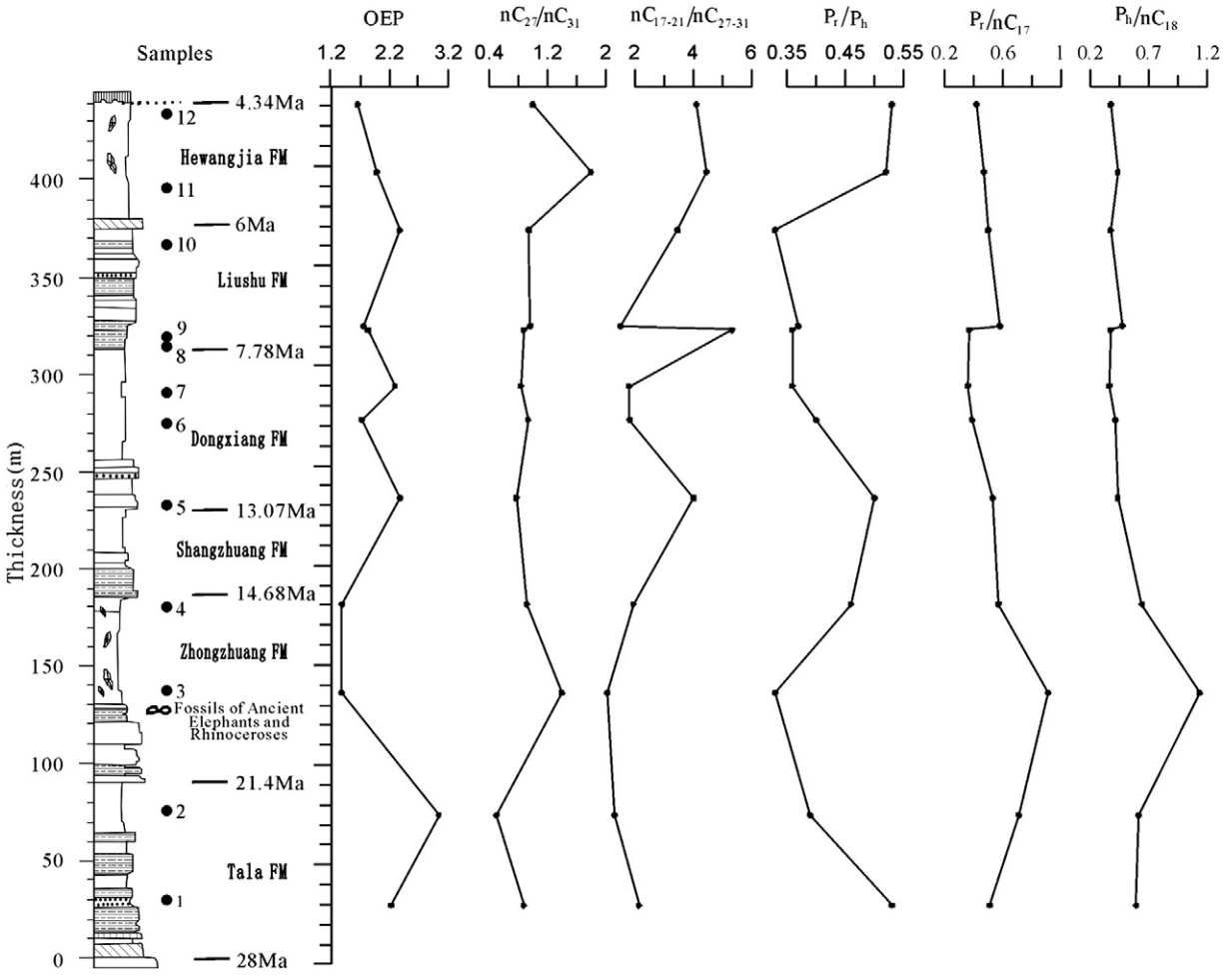

Fig. 4. Variations of various geochemistry parameters of n-alkanes in study section.

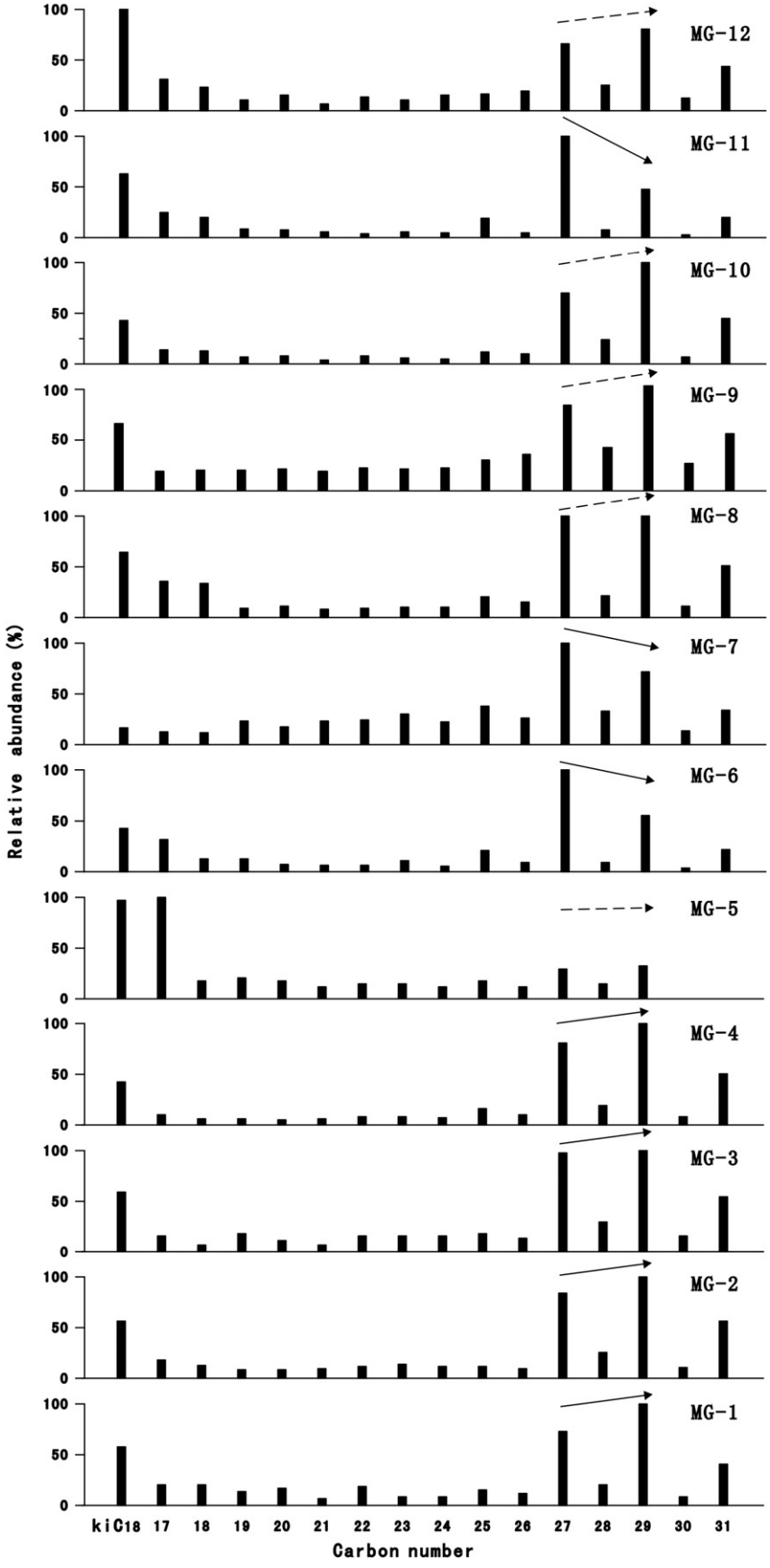

Fig. 5. The distribution of n-alkan-2-one in all samples.

important contributions of aquatic plant waxes, which is consistent with the palynological data that indicate that this sample is from the wettest portion of the paleoclimate history of this rock sequence. The fossils of giant mammals, such as ancient elephants and rhinoceroses, therefore, appeared accordingly in MG3 at ~18.4 Ma (Fig. 2).

As shown in Table 1, the ratio of pristine (Pr) to phytane (Ph) in all samples was within the range of 0.35 to 0.55. These values are thought to be due to a sub-oxic environment, which is possibly favorable for reducing conditions in the lacustrine sediments.

The time-resolved variability in the biomarker distributions in a sedimentary core from the Guadiana estuary provides a good result of the Pr/Ph ratio variations, which are always smaller than 1. These low values suggest that anoxic conditions in the active sediment layer prevailed at the very early stage of diagenesis. The C17/Pr and C18/Ph values < 1 throughout the core are also indicators of strong microbial activity (Gonzalez-Vilia et al., 2003). As shown in Fig. 4, the changes in the two ratios are approximately the same throughout the section. An obvious increase in the average ratios of Pr/nC_{17} and Ph/nC_{18} in our samples from top to bottom suggests that the microbial activity was strong and low-carbon-numbered alkanes were rich at the top of the section. Relatively high ratios in the bottom section indicate that the microbial activity was weak and high-carbon-numbered alkanes were rich.

In organic geochemistry, the carbon preference index (CPI) is used to indicate the degree of diagenesis of straight-chain geolipids; it is a numerical representation of how much of the original biological chain-length specificity is preserved in geological lipids (Meyers and Ishiwatari, 1995). Biomarkers from different biological origins have different CPI values. For instance, n-alkanes from the cuticular waxes of higher plants have a strong odd/even predominance and give high CPI values (> 5), whereas n-alkanes from bacteria and algae show a weak odd/even predominance and give low CPI values (~1) (Cranwell et al., 1987). The CPI values of n-alkanes can indicate the maturity of organic matter. As shown in Table 1, the CPI_{23-31} values in all samples are low (ranging from 1.26 to 2.01), with an average of 1.59. This result indicates a moderate maturity of the organic matter, which might have originated directly from autochthonous organic matter input of the fluvial and lacustrine sediments in the Maogou section.

4.2. Distribution of n-alkenones and climate significance

Alkyl-ketones are considered significant biomarkers of environment and biogenesis. The different biological origins of these biomarkers indicate different climate and environmental conditions, so changes in the distribution of alkyl-ketones can reveal changes in climate, which has been demonstrated for a variety of natural systems. The research targets have included marine and lacustrine sediments (Cranwell 1977; Albaiges et al., 1984; Meyer and Ishiwatari, 1993), soils (Huang et al., 1996; Jaffe et al., 1996; Bull et al., 2000; Wang et al., 2003; Naafs et al., 2004), peats (Lehtonen and Ketola, 1990; Nott et al., 2000), paleosols (Freeman and Colarusso, 2001; Wang et al., 2002) and aerosols (Simoneit et al., 1988, 1991; Zheng et al., 1997).

Abundant n-alkan-2-one compounds were detected in all samples, and their distribution ranged from C_{17} to C_{31}. The maxima peaks of C_{27}, C_{29} and C_{31} were especially obvious, and the predominance of odd carbon numbers was remarkable from C_{25} to C_{31} (Fig. 5). The distribution of n-alkan-2-ones in most samples is similar to that of n-alkanes, exhibiting an evident odd carbon predominance in C25–C35. This result may suggest that the pathway from alkanes to alkanones is the n-alkanes by alpha oxidation of the carbon chains.

As shown in Fig. 5, the maxima peaks of n-alkan-2-one from relatively higher to lower carbon-numbered compounds changed in accordance with the six stages. The first stage was for MG1 to MG4, with a main peak predominance of C_{29} and a secondary peak predominance of C_{27} from ~25.8 Ma to ~15.3 Ma. The second stage was in MG5, with C_{29} being the predominant peak and C_{27} being the secondary peak, suggesting that the predominant contribution to the sediments changed at ~13 Ma. The third stage was for MG6 to MG7, with C_{27} as the predominant peak and with the C_{29} secondary peak from ~10 Ma to ~9 Ma. The fourth stage was for MG8 to MG10, with C_{29} as the major peak and C_{27} as the secondary peak from ~8 Ma to ~6.25 Ma. The fifth stage was in MG11, with the main peak predominance of C_{27} and the secondary peak predominance of C_{29} at ~5.5 Ma. The sixth stage was in MG12, with the main peak predominance of C_{29} and secondary peak predominance of C_{27} at ~4.5 Ma.

Abundant isoprene-ketones (i.e., isomeric C18 ketones, iKC18, Fig. 5) were detected in all samples. The relative abundance of isoprene-ketones for MG5 and MG8 to MG11 was higher, whereas those for MG1 to MG4 and MG6 to MG7 were low. The isoprene-ketones are likely related to the temperature changes in the sedimentary environment. A higher abundance of isoprene-ketones may indicate a lower temperature in the sedimentary environment. The greatest change was for MG7 to MG8, where the relative abundance of isoprene-ketones increased sharply, which indicates that the climate suddenly turned toward cold conditions at ~8 Ma. Another obvious change in the relative abundance of isoprene-ketones was found in the higher amounts in MG5, which indicates cold conditions at ~13 Ma.

All of the above stages are likely to impart some information about early depositional conditions. These stages may record information about diagenetic conditions and processes in the sedimentary environment, which might be valuable for paleoclimate interpretations. Nevertheless, the origin of these compounds and their paleoclimate significance remains ambiguous, deserving further investigation.

5. Conclusions

The lacustrine sediments of the Maogou section of the east Linxia Basin were rich in organic compounds. Biomarkers such as n-alkanes, isoprenoids and n-alkyl-ketones were detected in all the samples. Our results show that molecular fossils in the Maogou section record the process of arid environment change and the climate response to the uplift of the Tibetan Plateau. These results are similar to the record of climate change based on the study of palynofloras. The main observations from this study are summarized as follows:

1. The characteristic bimodal distribution of *n*-alkanes, which was observed in the investigated samples, is centered on *n*-C_{17}–*n*-C_{20} and has maximum values at *n*-C_{18} in all samples; and *n*-C_{27}–*n*-C_{31} has maximum values at *n*-C_{29} in some of the samples. The front mode shows a weak even-carbon-number predominance of short-chain *n*-alkanes (CPI_{17-21} 0.55–0.89); in contrast, the back mode has a strong odd-carbon-number predominance of long-chain *n*-alkanes (CPI_{25-31} 1.41–2.42).
2. The distribution of n-alkanes is characterized by a striking increase in the high-carbon-numbered n-alkanes at ~13 Ma and ~8 Ma, which suggests large inputs of higher plants when the climate changed toward cold and arid conditions. This result is similar to the record of slight temperature decrease and aridification events based on the study of palynofloras.
3. The ratios of $(nC_{17}–nC_{21})/(nC_{27}–nC_{31})$ show six stages of climate change throughout the entire depositional section and a distinct change to a dry climate at ~8 Ma. The results again agree with previous observations based on the study of palynofloras. The ratio of n-alkane nC_{27}/nC_{31} (woody plants/grassy plants) reflected three climatic stages throughout the entire depositional section. The maximum ratios for MG3 and MG11 at ~18.4 Ma and ~5.5 Ma, respectively, suggest that there are two major humid stages of climatic change in the whole section, which are similar to the events of the warmest and most humid periods based on

palynofloras. Therefore, the fossils of giant mammals, such as the ancient elephants and rhinoceroses, appeared accordingly at ~18.4 Ma.

4. The ratio of pristine (Pr) to phytane (Ph) in all samples suggests that the environments in the lacustrine sediments were possibly favorable for reductive processes. The ratios of Pr/nC_{17} and Ph/nC_{18} indicate strong and weak microbial activities, respectively. The CPI_{23-31} values of the n-alkanes exhibit a moderate maturity of the organic matter, which might have originated directly from autochthonous organic matter input of the fluvial and lacustrine sediments in the Maogou section.
5. The different maxima peaks of n-alkan-2-ones changed from relatively higher- to lower-carbon-numbered compounds in the context of the six climate stages. The abundance of isoprene-ketones (iKC_{18}) in the section recorded the changes in temperature in the sedimentary environment.

Acknowledgments

We thank Engineer Wanren Ding for providing analytical assistance with the extraction of hydrocarbon fractions. We thank Dr. Brian Jones and an anonymous reviewer who refereed and provided helpful comments for this paper.

References

Albaiges, J., Algaba, J., Grimalt, J., 1984. Extractable and bound neutral lipids in some lacustrine sediments. Organic Geochemistry 6, 502–507.
An, Z.S., Kutzbach, J.E., Prell, S.C., 2002. Evolution of Asian monsoons and phrased uplift of the Himalaya-Tibetan plateau since Late Miocene times. Nature 411, 62–66.
Bai, Y., Fang, X.M., Wang, Y.L., Kenig, F., 2006a. Features of aliphatic ketones and their environmental significance in modern soils of various climate regions. Organic Geochemistry 37, 640–646.
Bai, Y., Fang, X.M., Wang, Y.L., 2006b. Branched alkanes with quaternary carbon atoms in Chinese soils: potential environmental implications. Chinese Science Bulletin 51 (1), 1–8.
Bull, I.D., van Bergen, P.F., Nott, C.J., Poulton, P.R., Evershed, R.P., 2000. Organic geochemical studies of soils from the Rothamsted classical experiments–V. The fate of lipids in different long-term experiments. Organic Geochemistry 31, 389–408.
Cranwell, P.A., 1977. Organic geochemistry of Cam Loch (Sutherland) sediments. Chemical Geology 20, 205–221.
Cranwell, P.A., Eglinton, G., Robinson, N., 1987. Lipids of aquatic organis ms as potential contributors to lacustrine sediments II. Organic Geochemistry 11 (6), 513–527.
Dettman, David L., Fang, X.M., Garzione, Carmala N., Li, J.J., 2003. Uplift-driven climate change at 12 Ma: a long $\delta^{18}O$ record from the NE margin of the Tibetan plateau. Earth and Planetary Science Letters 214, 267–277.
Ding, Z.L., Xiong, X.F., Sun, J.M., Yang, S.L., Gu, Z.Y., Liu, T.S., 1999. Pedostraigraphy and paleomagnetism of a 7.0 Ma eolian loess-red clay sequence at Lingtai, Loess Plateau, north-central China and the implications for paleomosoon evolution. Paleogeography, paleoclimatology, palaeoeclogy 152, 49–66.
Evershed, R.P., Dudd, S.N., Charters, S., 1999. Lipids as carriers of anthropogenic signals from prehistory. Philosophical Transactions of the Royal Society of London 354, 19–31.
Fang, X.M., Ono, Y., Fukusawa, H., 1999. Asian summer monsoon instability during the past 60000 years:magnetic susceptibility and pedogenic evidence from the western Chinese Loess Plateau. Earth and Planetary Science Letters 168, 219–232.
Fang, X.M., Carmala, G., Van der, V.R., 2003. Flexual subsidence by 29 Ma on the NE edge of Tibet from the magnetostratigraphy of linxia Basin, China. Earth and Planetary Science Letters 210, 545–560.
Freeman, K.H., Colarusso, L.A., 2001. Molecular and isotopic records of C4 grassland expansion in the late Miocene. Geochimica et Cosmochimica Acta 65, 1439–1454.
Fu, J.M., Sheng, G.Y., 1992. Molecular organic geochemistry and its application to the staudy of paleoclimate and paleoenvironments. Quaternary Sciences 4, 306–320.
Fu, J.M., Sheng, G.Y., 1996. Preliminary study on environmental organic geochemistry. Earth Science Frontier 3, 127–132.
Gonzalez-Vilia, F.J., Polvillo, O., Boski, T., Moura, D., de Andres, J.R., 2003. Biomarker patterns in a time-resolved holocene/terminal Pleistocene sedimentary sequence from the Guadiana river estuarine area (SW Portugal/Spain border). Organic Geochemistry 34, 1601–1613.
Greenwood, P.F., Arouri, K.R., 2003. Abundance and geochemical significance of C-2n dialkylalkanes and highly branched C-3n alkanes in diverse Meso- and Neoproterozoic sediments. Organic Geochemistry 35, 331–346.
Guo, Z.T., Ruddiman, W.F., Hao, Q.Z., Wu, H.B., Qiao, Y.S., Zhu, R.X., Eng, S.Z., Wei, J.J., Yuan, B.Y., Liu, T.S., 2002. Onset of Asian desertification by 22 Myr ago inferred from loess deposits in China. Nature 416, 159–163.
Huang, Y., Bol, R., Harkness, D.D., Ineson, P., Eglinton, G., 1996. Post-glacial variations in distributions, ^{13}C and ^{14}C contents of aliphatic hydrocarbons and bulk organic matter in three types of British acid upland soils. Organic Geochemistry 24, 273–287.
Jaffe, R., Elisme, T., Cabrera, A.C., 1996. Organic geochemistry of seasonally flooded rain forest soils: molecular composition and early diagenesis of lipid components. Organic Geochemistry 25, 9–17.
Lehtonen, K., Ketola, M., 1990. Occurrence of long-chain acyclic methyl ketones in Sphagnum and Carex peats of various degress of humification. Organic Geochemistry 15, 275–280.
Li, J.J., 1995. Uplift of Qinghai-Xizang (Tibet) Plateau and Global Change. Lanzhou University Press, Lanzhou, p. 207.
Li, J.J., Fang, X.M., 1998. Uplift of Qinghai-Tibetan Plateau and environmental change. Chinese Science Bulletin 43 (15), 1569–1574.
Lu, B., Chen, R.H., Zhou, H.Y., 2005. Oceanic environmental changes of subarctic Bering Sea in recent 100 years: evidence from molecular fossils. Science in China Series D: Earth Sciences 48 (4), 555–564.
Ma, Y., Li, J., Fan, X., 1998. Pollen-based vegetational and climatic records during 30.6 to 5.0 My from Linxia area, Gansu. Chinese Science Bulletin 43 (3), 301–304.
Meyer, P.A., Ishiwatari, R., 1993. Lacustrine organic geochemistry: an overview of indicators of organic matter sources and diagnesis in lake sediments. Organic Geochemistry 20 (7), 867–900.
Meyers, P.A., Ishiwatari, R., 1995. Organic matter accumulation records in lake sediments. In: Lerman, A., Imboden, D.M., Gat, J.R. (Eds.), Physics and Chemistry of Lakes. Springer, Berlin, pp. 279–328.
Mitra, S., Bianchi, T.S., Guo, L., 2000. Terrestrially derived dissolved organic matter in the Chesapeake Bay and the Middle Atlantic Bight. Geochimca et Cosmochimica Acta 64, 3547–3557.
Naafs, D., Van Bergen, P.F., Boogert, S.J., de Leeuw, J.W., 2004. Solvent-extractable lipids in an acid andic forest soil; variations with depth and season. Soil Biology and Biochemistry 36, 297–308.
Nott, C.J., Xie, S.C., Avsejs, L.A., Maddy, D., 2000. n-Alkane distributions in ombrotrophic mires as indicators of vegetation change related to climatic variation. Organic Geochemistry 31, 231–235.
Pearson, A., Mcnichol, A.P., 2001. Origins of lipid biomarkers in Santa Monica Basin surface sediment: a case study using compound-specific $\triangle^{14}C$ analysis. Geochimca et Cosmochimica Acta 65 (18), 3123–3137.
Sheng, G.Y., Cai, K.Q., Yang, X.X., 1999. Long-chain alkenones in Hotong Qagan Nur Lake sediments and its paleoclimatic implications. Chinese Science Bulletin 44 (3), 259–260.
Simoneit, B.R.T., Cox, R.E., Standley, L.J., 1988. Organic matter of the troposphere-IV: lipids in harmattan aerosols of Nigeria. Atmospheric Environment 22, 983–1003.
Simoneit, B.R.T., Sheng, G.Y., Chen, X.J., Fu, J.M., Zhang, J., Xu, Y.P., 1991. Molecular marker study of extractable organic matter in aerosols from urban areas of China. Atmospheric Environment 25 (10), 2111–2119.
Song, G.Y., Fang, X.M., Li, J.J., 2001. The Late Cenozoic uplift of the Liupan Shan, China. Series D:Earth Sciences 31, 142–148.
Street Perrott, F.A., Huang, Y., Perrott, A., 1997. The impact of lower atmospheric CO_2 on tropical mountain ecosystems. Science 278, 1422–1426.
Sun, D.H., Chen, M.Y., JohnShow, Lu, H.Y., Sun, Y.B., Yue, L.P., Zhang, Y.X., 1998. Magnetostratigraphy and paleoclimate records of Late Cenozoic Eolian Sequence in the Loess Plateau of China. Science in China Series D:Earth Sciences 28 (1), 79–84.
Thiel, V., Jenisch, A., Landmann, G., 1997. Unusual distributions of long-chain alkenones and tetraahymanol from the highly alkaline Lake Van, Turkey. Geochimica et Cosmochimica Acta 61 (10), 2053–2064.
Volkman, J.K., Barrett, S.M., Blackburn, S.I., 1995. Allkenones in gephyrocapsa oceanica: implications for studies of paleoclimate. Geochimca et Cosmochimica Acta 59, 513–520.
Wang, Y., Deng, T., 2005. A 25 m.y. isotopic record of paleodiet and environmental change from fossil mammals and paleosols from the NE margin of the Tibetan Plateau. Earth and Planetary Science Letters 236, 322–338.
Wang, Z.Y., Yu, J.H., Gu, Y.S., Lv, C.Y., Yi, Y., Xie, S.C., 2002. Molecular fossils as indicators for paleo-environment fromQuaternary red earth in Changing, Zhejiang. Marine Geology and Quaternary Geology 22, 97–102.
Wang, Z.Y., Liu, Z.H., Yi, Y., Xie, S.C., 2003. Features of lipids and their implications in modern soils from various climate vegetation regions. Acta Pedologica Sinica 40, 967–970.
Wang, Z.Y., Xie, S.C., Chen, F.H., 2004. n-Alkane distribution as indicator for paleovegetation an example from Yangbao S1 paleosol in Linxia, Gansu province. Quaternary Sciences 24 (2), 231–235.
Wang, Y.L., Wang, X.B., Wang, Y.X., 2005. The analysis of biomarkers in modern lake sediments from antractica with supercritical fluid extraction and gas chromatography–mass spectrometry. Chinese Journal of Analytical Chemistry 33 (2), 289.
Wang, Y.L., Fang, X.M., Bai, Y., 2006. Macrocyclic alkanes in modern soils of China. Organic Geochemistry 37, 146–151.
Wang, Y.L., Fang, X.M., Bai, Y., 2007. Distribution of lipids in modern soils from various regions with continuous climate (moisture-heat) change in China and their climate significance. Science in China Series D: Earth Sciences 50 (4), 600–612.
Xie, S.C., Evershed, R.P., 2001. Peat molecular fossils recording paleoclimatic matter in replacement. Chinese Science Bulletin 46 (20), 1749–1752.
Xie, S.C., Yao, T.D., Kang, S.C., 1999. Climatic and environmental implications from organic matter in Dasuopu glacier in Xixiabandma in Qinghai–Tibetan Plateau. Science in China Series D:Earth Sciences 42 (4), 383–391.
Xie, S.C., Wang, Z.Y., Wang, H.M., 2002. The occurrence of a grassy vegetation over the Chinese Loess Plateau since the last interglacier: the molecular fossil record. Science in China Series D:Earth Sciences 45 (1), 53–62.
Xie, S.C., Chen, F.H., Wang, Z.Y., 2003a. Lipid distribution in loess-paleosol sequences from Northwest China. Organic Geochemistry 34 (8), 1071–1079.
Xie, S.C., Yi, Y., Huang, J.H., 2003b. Lipid distribution in a subtropical southern China stalagmite as a record of soil ecosystem response to paleolimate change. Quaternary Sciences 60, 340–347.

Xie, S.C., Yi, Y., Liu, Y.Y., 2003c. The Pleistocene vermicular red earth in South China signaling the global climatic change: the molecular fossil record. Science in China Series D:Earth Sciences 33 (5), 411–417.
Yan, B.Z., Jia, R.F., Hu, K., 1998. Distribution of chain hydrocarbon from weinan loess section and their paleoclimatic significance. Geochimica 27 (2), 180–186.
Zhang, G., Sheng, G.Y., Fu, J.M., 1999. Molecular organic geochemical evidence for paleoenvironmental changes at 11.87-12.28 m in GS-1 sedimentary core, Gucheng Lake. East China[J]. Chinese Science Bulletin 44 (15), 1407–1411.
Zhang, H.C., Chang, F.Q., Li, B., Lei, G.L., Chen, Y., Zhang, W.X., Niu, J., Fan, H.F., Yang, M.S., 2007. Brached aliphatic alkanes of shell bar section in Qarhan lake, Qaidam Basin and their paleoclimate significance. Chinese Science Bulletin 52 (9), 1248–1256.
Zheng, M., Wan, T.S.M., Fang, M., Wang, F., 1997. Characterization of the non-volatile organic compounds in the aerosols of Hong Kong-identification, abundance and origin. Atmospheric Environment 31, 227–237.